THE JOURNAL OF PHYSICAL CHEMISTRY Letters

pubs.acs.org/JPCL

Ground-State Depletion Microscopy: Detection Sensitivity of Single-Molecule Optical Absorption at Room Temperature

Shasha Chong,[‡] Wei Min,[†,‡] and X. Sunney Xie*

Department of Chemistry and Chemical Biology, Harvard University, Cambridge, MA 02138, United States

ABSTRACT Optical studies of single molecules in ambient environments, which have led to broad applications, are primarily based on fluorescence detection. Direct detection of optical absorption with single-molecule sensitivity at room temperature is difficult because absorption is not a background-free measurement and is often complicated by sample scattering. Here we report ground-state depletion microscopy for ultrasensitive detection of absorption contrast. We image 20 nm gold nanoparticles as an initial demonstration of this microscopy. We then demonstrate the detection of an absorption signal from a single chromophore molecule at room temperature. This is accomplished by using two tightly focused collinear continuous-wave laser beams at different wavelengths, both within a molecular absorption band, one of which is intensity modulated at a high frequency (> MHz). The transmission of the other beam is found to be modulated at the same frequency due to ground state depletion. The signal of single chromophore molecules scanned across the common laser foci can be detected with shot-noise limited sensitivity. This measurement represents the ultimate detection sensitivity of nonlinear optical spectroscopy at room temperature.

SECTION Kinetics, Spectroscopy

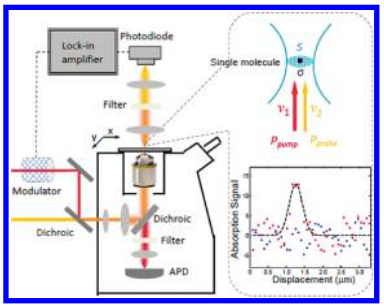

Single-molecule optical detection, imaging, and spectroscopy have had an impact on many disciplines.[1−5] In particular, room temperature optical detection of single molecules has been used extensively in biological research.[3−5] Single-molecule optical detection at room temperature dates back to 1976 when Hirschfeld reported the use of an optical microscope to reduce probe volume, and hence the background signal.[6] He was able to detect individual immobilized protein molecules labeled with tens of fluorophores, demonstrating a single-molecule line-scan image. Similar use of optical microscopes finally allowed single fluorophore sensitivity at room temperature in 1990.[7,8] It has remained the method of choice for detecting and imaging single molecules in ambient environments to the present.

Among the methods that subsequently emerged, single chromophore detection was first achieved by optical absorption measurement at 1.6 K with a sophisticated frequency modulation scheme in 1989.[9] This measurement relied on the large absorption cross-section of the zero-phonon line. It was soon followed by fluorescence detection via excitation at the zero-phonon line, which offered much higher sensitivity by virtue of background free emission detection.[10] These methods, however, were limited only to cryogenic temperatures at which zero-phonon lines exist for a handful of molecules.

Imaging of single fluorophores at room temperature was first accomplished with near-field microscopy in 1993.[11] Although a seminal contribution, near-field single molecule imaging had limited applications because of the complexity and perturbation of the near-field probes, and was soon surpassed by much easier far-field single molecule imaging with total internal reflection[12] and confocal microscopy.[1,13]

Surface enhanced Raman scattering is capable of detecting single molecules,[14,15] but it requires close contact of molecules with a metal nanostructure, which is difficult to control. High-sensitivity measurements toward single-molecule spectroscopy have been attempted with other contrasts besides fluorescence and Raman scattering, including interferometry,[16,17] stimulated emission,[18] photothermal[19,20] and direct absorption measurements.[21] The photothermal method has recently reached single-molecule sensitivity;[22] however, glycerol, an uncommon solvent, was used in order to reduce heat conductivity and increase the refractive index change induced by single-molecule light absorption. The direct absorption method has recently demonstrated single molecule sensitivity.[21] By careful selection of the sample substrate, the authors avoided the major complication of sample scattering for direct absorption measurements. We seek a different approach for detection of single-molecule optical absorption at room temperature.

Received Date: October 18, 2010
Accepted Date: October 22, 2010
Published on Web Date: November 11, 2010

DOI: 10.1021/jz1014289 | *J. Phys. Chem. Lett.* **2010**, *1*, 3316–3322

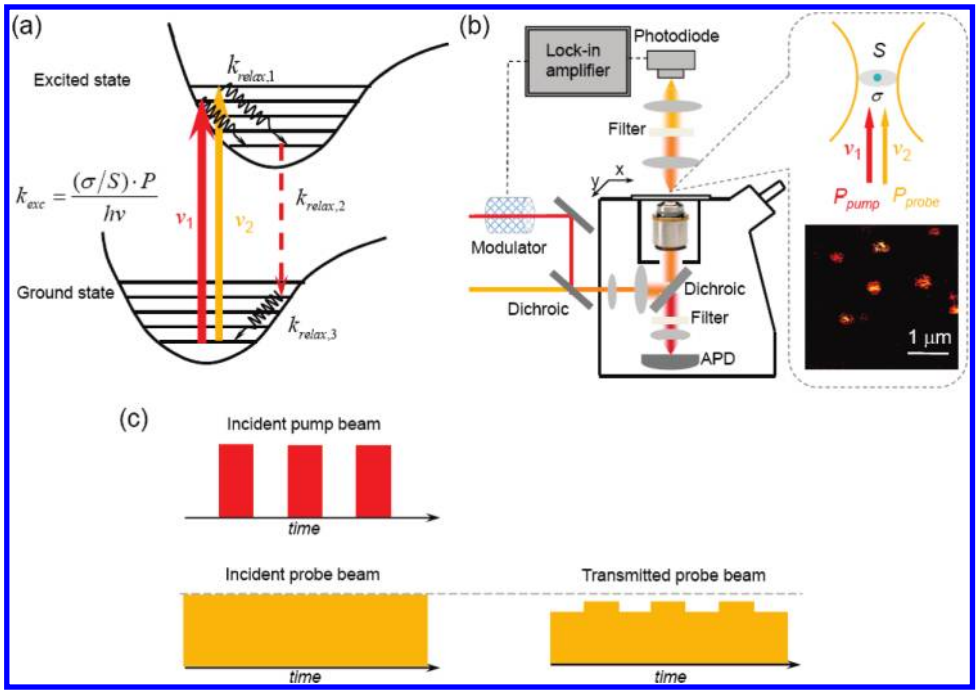

Figure 1. (a) Energy diagram for optical absorption, excited-state relaxation, and ground-state depletion of a molecule. Laser fields ν_1 and ν_2 are both on resonance with the absorption of the molecule. One beam affects the absorption of the other beam by depleting the ground state of the molecule. (b) Experimental setup for the simultaneous ground state depletion and epi-fluorescence detection. The inset indicates single-molecule absorption cross section σ and the cross section of a tightly focused laser beam S. It also shows a fluorescence image of single molecule Atto647N embedded in PMMA. (c) Schematic diagram of modulation transfer based on ground-state depletion. As the intensity of the pump beam is modulated on and off over time, the probe beam is also modulated at the same frequency.

Recently, several nonlinear optical imaging techniques including stimulated Raman scattering microscopy,[23] two-photon absorption microscopy,[24] and stimulated emission microscopy[18] have been developed for imaging nonfluorescent species. The nonlinearity of these techniques allows three-dimensional sectioning. The techniques use two pulse laser trains of different wavelengths, which coincide in the sample. The first beam is intensity modulated at a high frequency (> MHz), while the second beam is monitored by a photodetector via phase sensitive detection with a lock-in amplifier. As a result of nonlinear interactions between the two laser beams and the sample, the transmission of the second beam is modulated at the same frequency as the first beam. The high-frequency modulation transfer method effectively circumvents laser intensity fluctuations and the intensity variation of a transmitted laser beam that is scanned across a heterogeneous sample, both of which occur at low frequencies (direct current to kilohertz). Here we demonstrate ground-state depletion microscopy with CW lasers that offers single-molecule sensitivity for detection of optical absorption, but is free from sample scattering complications.

Consider the ground state and excited state of a molecule (Figure 1a); the attenuated power of the incident beam P by the single molecule at the laser focus is (see Supporting Information for derivation)

$$\Delta P = \frac{k_{\text{relax}} \cdot (\sigma/S) \cdot P}{k_{\text{relax}} + (\sigma/h\nu S) \cdot P} \qquad (1)$$

where k_{relax} is the $k_{\text{relax},2}$ in Figure 1a, which is the rate constant of the rate-limiting step in the sequential relaxation process from the vibronic states prepared by the optical excitation to the lowest vibrational level in the ground electronic state. $h\nu$ is the photon energy, σ is the absorption cross-section for a single chromophore ($\sim 10^{-16}$ cm^2 at room temperature), and S is the beam waist area ($\sim 10^{-9}$ cm^2). The relative light attenuation, $\Delta P/P$, is no more than 10^{-7}–10^{-6} for a single molecule at room temperature. Conventional single-beam absorption microscopy cannot detect such a small attenuation, as it would be buried in the laser intensity noise (~1 %). Moreover, Rayleigh scattering due to the inhomogeneous refractive index of the sample also contributes to the attenuation.

We employ the modulation transfer detection scheme to measure ground-state depletion in a pump–probe experiment (Figure 1a,b). Two continuous-wave (CW) lasers, a pump beam at frequency ν_1 and a probe beam at frequency ν_2, are both on resonance with the same absorption band of the molecule. The incident power levels of pump and probe beams, P_{pump} and P_{probe}, are adjusted to be near the saturation intensity of the absorption transition. We modulate the incident intensity of the pump beam ν_1 at 1.75 MHz, and keep the incident intensity of the probe beam ν_2 constant (Figure 1c). The collinearly propagating pump and probe beams are focused to a common spot. The sample is scanned across the fixed laser foci with a piezoelectric scanning stage (Figure 1b). After passing through the sample, the transmitted

DOI: 10.1021/jz1014289 | J. Phys. Chem. Lett. 2010, 1, 3316–3322

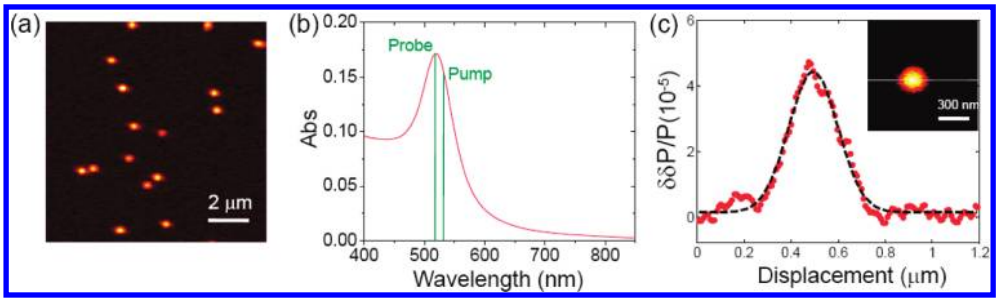

Figure 2. (a) Ground-state depletion imaging of single 20 nm gold nanoparticles. (b) Ensemble absorption spectrum of 20 nm gold nanoparticles in aqueous solution. The wavelengths of pump beam (532 nm) and probe beam (520 nm) are indicated. (c) Signal intensity profile of a single nanoparticle. The inset is the ground-state depletion image of the nanoparticle whose signal intensity profile is plotted as (c). The lateral position of (c) is indicated.

probe beam is detected by a photodiode while the pump beam is blocked by a filter. The photodiode signal is demodulated by a lock-in amplifier to create the ground-state depletion contrast. The modulation depth of the transmitted probe beam is

$$\delta\delta P_{\text{probe}} = \frac{2k_{\text{relax}} \cdot (\sigma^2/S^2 h\nu) \cdot P_{\text{pump}} P_{\text{probe}}}{(k_{\text{relax}} + (\sigma/h\nu S) \cdot P_{\text{probe}}) \cdot (k_{\text{relax}} + (\sigma/h\nu S) \cdot (2P_{\text{pump}} + P_{\text{probe}}))} \quad (2)$$

(see Supporting Information for derivation).

As an initial demonstration of ground-state depletion microscopy, we imaged individual 20 nm gold nanoparticles dispersed on a glass surface (Figure 2a), whose absorption spectrum is shown in Figure 2b along with the pump and probe wavelengths. The power level at focus was 450 μW for each beam. The pixel dwell time was 6.5 ms, and the time constant of the lock-in amplifier was set as 3 ms. Figure 2c shows the diffraction-limited intensity profile for a single nanoparticle in the inset image, which reveals a signal of $\delta\delta P/P \sim 0.5 \times 10^{-4}$, where P refers to the probe beam power at the photodiode. We assigned the signal detected to ground state depletion.

This assignment is supported by a calculation of the ground-state depletion signal for a single gold nanoparticle. The absorption cross section of a 20 nm gold nanoparticle at its plasmon resonance is $\sim 4 \times 10^{-12}$ cm^2.[25] Time-resolved measurement shows that the bleached ground state recovers sequentially through a fast electron−phonon relaxation (1−4 ps)[26,27] and a slow phonon−phonon relaxation (~100 ps).[27] The ground state recovery kinetics has been shown to be biexponential with the slow component having ~10% weight.[26] Under the condition of our CW excitation, the signal $\delta\delta P/P$ for a single gold nanoparticle is estimated to be $\sim 1 \times 10^{-4}$ (see Supporting Information). This theoretical estimation is comparable to our measured signal of $\delta\delta P/P \sim 0.5 \times 10^{-4}$ (Figure 2c).

An alternative explanation for the observed contrast is the photothermal effect, which has been used to image single gold nanoparticles.[25] It gives rise to refractive index variation at the laser foci, which could change the transmission of the probe beam while the pump beam is modulated, causing an apparent modulation transfer. However, the photothermal effect is known to increase with a decreasing modulation frequency due to more heat accumulation.[25] We found instead that our signal level is independent of modulation frequency (see Supporting Information). In addition, the thermal lens, when measured with modulation transfer, usually exhibits a 180° signal phase change as the position of the laser focus is scanned in the longitudinal direction.[28,29] We found that the signal is always in phase with the pump beam in a z-scan experiment. For these reasons, photothermal effects cannot explain the data in Figure 2.

For detecting single molecule absorption, we use an organic dye Atto647N, whose absorption spectrum is shown in Figure 3a. Wavelengths for pump and probe are 642 nm and 633 nm respectively. Fluorescence of the molecule is simultaneously collected and confocally detected.

The power dependence and sensitivity of ground state depletion microscopy were characterized with an aqueous solution of Atto647N in a pH 7 phosphate buffer. At low excitation intensity, eq 2 approaches

$$\delta\delta P = \frac{(2\sigma^2/S^2 h\nu) \cdot P_{\text{pump}} P_{\text{probe}}}{k_{\text{relax}}} \quad (3)$$

The inset of Figure 3b shows that the signal from an ensemble is linearly dependent on the product of pump and probe beam powers at low excitation intensities, consistent with eq 3. However, above saturation intensities, the linear curve becomes sublinear (Figure 3b). Note that the overall quadratic power dependence under nonsaturating conditions allows three-dimensional sectioning, as in many other multiphoton techniques.[18,30]

Figure 3c shows that the ground-state depletion signal depends linearly on the concentration of the Atto647N solution. This allows straightforward quantitative analysis. The best sensitivity is achieved under the condition that both pump and probe beams have near-saturation intensity levels: in our case, 350 μW for each beam at the focus. All further measurements were conducted at this power level. The detection limit is 15 nM with 1 s integration time, which corresponds to 0.3 molecule in the probe volume[31] ($\sim 3 \times 10^{-17}$ liter). The corresponding modulation depth, $\delta\delta P/P$, of a single Atto647N molecule is $\sim 0.9 \times 10^{-7}$. Note that the P in $\delta\delta P/P$ indicates the probe beam power at the photodiode. This measured result agrees with its

DOI: 10.1021/jz1014289 | J. Phys. Chem. Lett. 2010, 1, 3316–3322

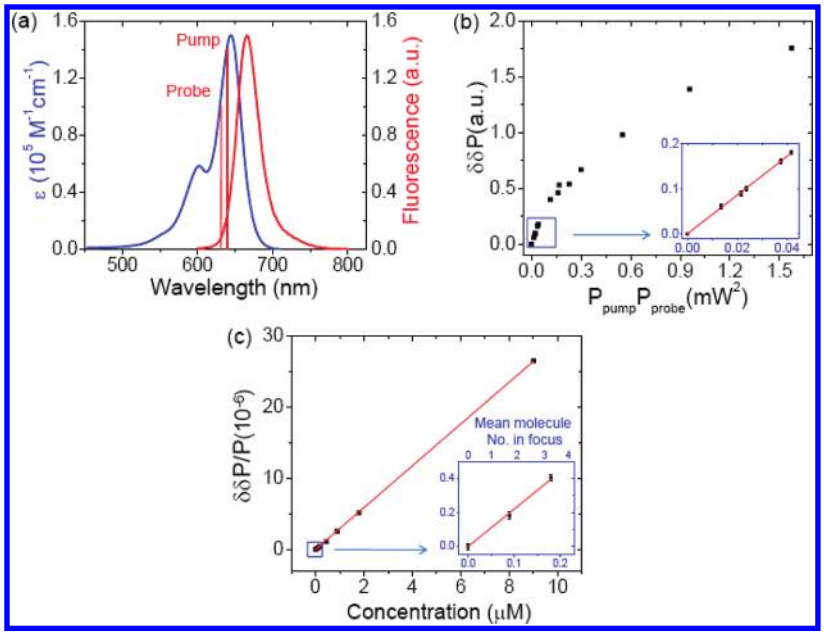

Figure 3. (a) Ensemble absorption and emission spectra of Atto647N in pH 7 aqueous solution. The wavelengths of pump and probe beams are indicated. (b) Ground depletion signal from 0.84 μM aqueous solution of Atto647N as a function of the product of pump beam power, P_{pump}, and probe beam power, P_{probe}. The blue frame indicates the linear portion of the function. The inset is a zoom-in of the blue frame of panel b. (c) Ground-state depletion signal as a function of concentration of aqueous Atto647N solution. The power level is 350 μW for each beam. The blue frame indicates the data points at lowest concentrations. The inset is zoom-in of the blue frame of (c), with concentrations labeled at the bottom and estimated mean molecule numbers in the probe volume labeled at the top. Error bars are for 1s integration time, indicating that single-molecule sensitivity is reachable.

theoretical value of $\sim 1.2 \times 10^{-7}$ based on eq 2 (see Supporting Information).

The inset of Figure 1b depicts a fluorescence image of single-molecule Atto647N embedded in a poly(methyl methacrylate) (PMMA) matrix. The blinking of fluorescence and one-step photobleaching clearly proves that the spot is from a single molecule. Lateral line scans across the maximum of the diffraction-limited spot were repeated, and the ground-state depletion and epifluorescence signals were recorded simultaneously. The time constant of the lock-in amplifier was 30 ms.

Figures 4a–d show the simultaneous line-scan signals of fluorescence and absorption of two single molecules. For molecule A, the fluorescence line scan signal as a function of time is shown in the inset of Figure 4a. It survived for 45 line scans before photobleaching (longer than the average survival lines of a single molecule; see Supporting Information). The red plots in Figure 4a,b show an average of 45 fluorescence and absorption line-scan signals before molecule A was photobleached. The lateral position of the peak value of $\delta\delta P/P \sim 1.4 \times 10^{-7}$ coincides with the peak position in the single molecule fluorescence line scan. This demonstrates the single-molecule sensitivity of the ground-state depletion microscope. The blue plot in Figure 4b shows that after molecule A was photobleached, an average of 45 absorption line-scan signals vanished. The detection of the absorption signal is shot-noise limited because the noise in Figure 4b is consistent with the estimated normalized shot noise $\Delta P/P \sim 3 \times 10^{-8}$ at the probe beam power used (see Supporting Information). Similar data for another molecule is shown in Figure 4c,d.

We note that ground-state depletion is not the only possible modulation transfer mechanism that could exist in such a pump–probe experiment. Excited-state absorption, stimulated emission, and photothermal effects might also cause intensity modulation of the probe beam. Had excited-state absorption been the underlying mechanism, we would expect a 180° phase difference between the detected signal and pump beam modulation.[32] We excluded this possibility because the detected signal is in phase with the pump beam modulation.

Stimulated emission would have the same phase as the ground-state depletion signal on the lock-in amplifier.[18] However, the probe wavelength is chosen to be shorter than the pump wavelength and is at the far edge of the emission spectra (Figure 3a). Therefore we do not expect stimulated emission to occur at the probe wavelength.

Our observed modulation transfer signal could also originate from the photothermal effect. Again, we exclude this by finding that our signal level is independent of modulation frequency (see Supporting Information) for Atto647N detection and that the signal is always in phase with the pump beam in a *z*-scan experiment.

In Figure 4e we report the distribution of the absorption signal from 130 molecules that survived more than 20 line scans. The single-molecule absorption signals $\delta\delta P/P$ are found to range from 4×10^{-8} to 2.6×10^{-7}, with a mean of 1.1×10^{-7}. This agrees well with the theoretical value expected from eq 2 (Figure 4e). The variation of $\delta\delta P/P$ can be explained by the random orientation of absorption dipole moments and the inhomogeneity of the single-molecule absorption spectrum.

The phenomena of ground-state depletion or nonlinear saturation spectroscopy has previously been used for super

DOI: 10.1021/jz1014289 | J. Phys. Chem. Lett. 2010, 1, 3316–3322

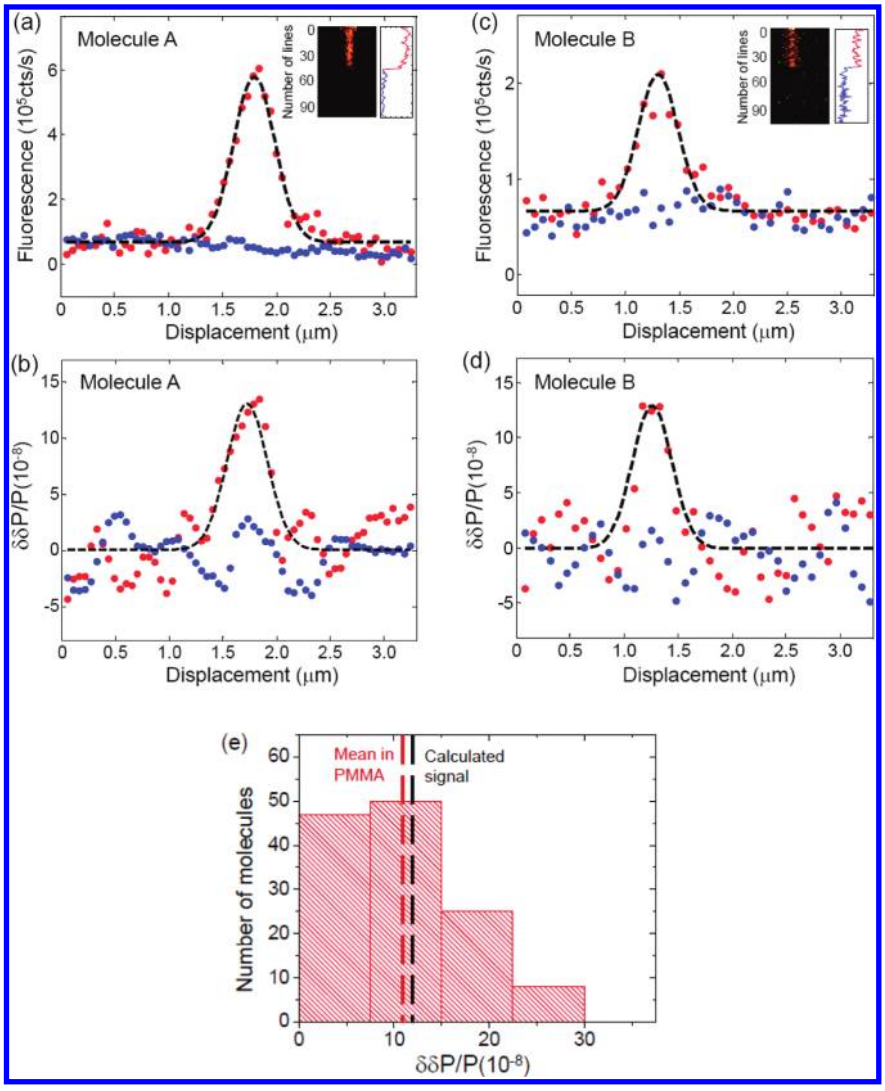

Figure 4. (a) Fluorescence line scans for molecule A, averaged from the inset before (red) and after (blue) photobleaching. The inset is the fluorescence image constructed from repeated line scans across molecule A and the corresponding fluorescence intensity trajectory. The molecule is photobleached after 45 line scans (39 ms per pixel). (b) Absorption line scans for molecule A, averaged before (red) and after (blue) photobleaching, simultaneously recorded with those in panel a. (c) Fluorescence line scans for molecule B, averaged from the inset before (red) and after (blue) photobleaching. The inset is the fluorescence image constructed from repeated line scans across molecule B and the corresponding fluorescence intensity trajectory. The molecule is photobleached after 44 line scans (78 ms per pixel). (d) Absorption line scans for molecule B, averaged before (red) and after (blue) photobleaching, simultaneously recorded with those in panel c. (e) Occurrence of absorption signals from 130 single Atto647N molecules. The mean is close to the theoretical value expected from eq 2.

resolution microscopy.[33,34] Here we employ it in a different way to provide a contrast mechanism for microscopy and high sensitivity in absorption-like measurements, which is free from the complication of Rayleigh scattering of the sample.

In conclusion, a high-frequency dual-beam modulation transfer scheme allows the ultimate sensitivity of nonlinear optical microscopy based on saturation spectroscopy: the detection of a single-molecule absorption signal at room temperature.

EXPERIMENTAL SECTION

For detection of 20 nm gold nanoparticles, a solid-state laser (Laser Quantum, Ventus VIS 532) at 532 nm is used as the pump beam, and a line of an argon−Krypton laser (Melles Griot, 643-AP-A01) at 520 nm is used as the probe beam. The polarizations of both lasers are parallel to each other. The intensity of the pump beam is modulated by an acoustic optical modulator (AOM, Crystal Technology, 3080−197) at 1.75 MHz. After spatial combination with a 50/50 beam splitter, the pump and probe beams collinearly propagate into an inverted microscope (Nikon, TE300). Both beams are focused to a common focal spot in the sample by a microscope objective (Olympus UPLANSAPO 100X, N.A. = 1.4). After passing through the sample, the transmitted probe beam is collected by another objective (Olympus TIRF, oil, 60X, N.A. = 1.45). While the pump beam is blocked by two bandpass filters (Semrock, FF01−520/15−25 and Chroma, ET510/25), the probe beam is detected by a photodiode (Thorlabs, PDA36A) operated at 10 dB gain. The output of

DOI: 10.1021/jz1014289 | J. Phys. Chem. Lett. 2010, 1, 3316–3322

the photodiode is filtered through a low pass filter (Mini Circuit, BLP-1.9+) before demodulation by a lock-in amplifier (Stanford Research Systems, SR844) to create the ground-state depletion contrast.

The single gold nanoparticle samples are prepared by spin-coating a gold colloid (Sigma-Aldrich, G1652) onto cleaned No. 1 microscope coverslips. A thin layer of polyvinyl alcohol (Aldrich, MW 31 000−50 000) is coated on top of the nanoparticles for blocking immersion oil and index-matching to maximize the collection efficiency of the probe beam into the detector. The sample is scanned across the fixed laser foci with a piezoelectric stage (Mad City Laboratories, Nano-H100) in $x-y$ dimension. A modified Nanoscope IIIA controller (Digital Instruments) is used for controlling the scanning stage and generating images by acquiring signals from the in-phase component output of the lock-in amplifier.

For detection of Atto647N molecules, a solid-state laser (CrystaLaser, DL640-050) at 642 nm is used as the pump beam, and a HeNe laser (Coherent, 31-2082-000) at 633 nm is used as the probe beam. The polarizations of both lasers are parallel to each other. The intensity of the pump beam is modulated at 1.75 MHz by the same AOM as for nanoparticle detection. The pump and probe beams are spatially combined with a dichroic mirror (Chroma, Q646LP-BS) and collinearly propagate into the same microscope as above. The scheme of generating the ground-state depletion signal is the same as that with the nanoparticle detection, except that the pump beam is blocked by a narrow bandpass filter (Semrock, LL01−633−12.5) while the probe beam is detected by the photodiode. Epifluorescence emitted by the molecules is spectrally filtered and collected by an avalanche photodiode (APD) (Perkin-Elmer, SPCM-CD2801) in confocal mode. The APD counts are read and converted to an analog signal by a gated photon counter (Stanford Research Systems, SR400). The Nanoscope IIIA controller is used for both generating fluorescence images by acquiring signals from the photon counter and recording ground-state depletion signals.

The single-molecule samples are prepared by spin-coating a 50 pM solution of Atto647N (Sigma-Aldrich, 04507) molecules (diluted into a PMMA matrix, 3% by mass PMMA, Polysciences, MW 75,000) onto cleaned No. 1 microscope coverslips. A thin layer of polyvinyl alcohol is coated on top of the PMMA layer.

SUPPORTING INFORMATION AVAILABLE Derivation of equations, calculation details of signal and noise, modulation frequency dependence of the ground-state depletion signal, single-molecule survival times, and detectability of single-molecule ground-state depletion signals. The material is available free of charge via the Internet at http://pubs.acs.org.

AUTHOR INFORMATION

Corresponding Author:

*To whom correspondence should be addressed. E-mail: xie@chemistry.harvard.edu.

Present Addresses:

† Current address: Department of Chemistry, Columbia University, New York, NY 10027, United States.

Author Contributions:

† These authors contributed equally to this work.

ACKNOWLEDGMENT We thank Sijia Lu, Maarten Roeffaers, and Peter Sims for helpful discussions, and Gary Holtom for help with lasers. This work was supported by the U.S. Department of Energy's Basic Energy Sciences Program (DE-FG02-09ER16104).

REFERENCES

(1) For review, see: Xie, X. S.; Trautman, J. K. Optical Studies of Single Molecules at Room Temperature. *Annu. Rev. Phys. Chem.* **1998,** *49*, 441–480.

(2) For review, see: Moerner, W. E.; Orrit, M. Illuminating Single Molecules in Condensed Matter. *Science* **1999,** *283*, 1670–1676.

(3) For review, see: Weiss, S. Fluorescence Spectroscopy of Single Biomolecules. *Science* **1999,** *283*, 1677–1683.

(4) For review, see: Selvin, P. R.; Ha, T. *Single Molecule Techniques*; Cold Spring Harbor Laboratory Press: Cold Spring Harbor, NY, 2007.

(5) For review, see: Xie, X. S.; Choi, P. J.; Li, G.; Lee, N. K.; Lia, G. Single-Molecule Approach to Molecular Biology in Living Bacterial Cells. *Annu. Rev. Biophys.* **2008,** *37*, 417–444.

(6) Hirschfeld, T. Optical Microscopic Observation of Single Small Molecules. *Appl. Opt.* **1976,** *15*, 2965–2966.

(7) Shera, B. E.; Seitzinger, N. K.; Davis, L. M.; Keller, R. A.; Soper, S. A. Detection of Single Fluorescent Molecules. *Chem. Phys. Lett.* **1990,** *174*, 553–557.

(8) Rigler, R.; Widengren, J. Ultrasensitive Detection of Single Molecules by Fluorescence Correlation Spectroscopy. *BioScience* **1990,** *3*, 180–183.

(9) Moerner, W. E.; Kador, L. Optical Detection and Spectroscopy of Single Molecules in a Solid. *Phys. Rev. Lett.* **1989,** *62*, 2535–2538.

(10) Orrit, M.; Bernard, J. Single Pentacene Molecules Detected by Fluorescence Excitation in a p-Terphenyl Crystal. *Phys. Rev. Lett.* **1990,** *65*, 2716–2719.

(11) Betzig, E.; Chichester, R. J. Single Molecules Observed by Near-Field Scanning Optical Microscopy. *Science* **1993,** *262*, 1422–1425.

(12) Funatsu, T.; Harada, Y.; Tokunaga, M.; Salto, K.; Yanagida, T. Imaging of Single Fluorescent Molecules and Individual ATP Turnovers by Single Myosin Molecules in Aqueous Solution. *Nature* **1995,** *374*, 555–559.

(13) Macklin, J. J.; Trautman, J. K.; Harris, T. D.; Brus, L. E. Imaging and Time-Resolved Spectroscopy of Single Molecules at an Interface. *Science* **1996,** *272*, 255–258.

(14) Nie, S.; Emory, S. R. Probing Single Molecules and Single Nanoparticles by Surface-Enhanced Raman Scattering. *Science* **1997,** *275*, 1102–1106.

(15) Kneipp, K.; Wang, Y.; Kneipp, H.; Perelman, L. T.; Itzkan, I.; Dasari, R. R.; Feld, M. S. Single Molecule Detection Using Surface-Enhanced Raman Scattering (SERS). *Phys. Rev. Lett.* **1997,** *78*, 1667–1670.

(16) Hwang, J.; Fejer, M. M.; Moerner, W. E. Scanning Interferometric Microscopy for the Detection of Ultrasmall Phase Shifts in Condensed Matter. *Phys. Rev. A* **2006,** *73*, 021802.

(17) Kukura, P.; Celebrano, M.; Renn, A.; Sandoghdar, V. Imaging a Single Quantum Dot When It Is Dark. *Nano Lett.* **2008,** *9*, 926–929.

(18) Min, W.; Lu, S.; Chong, S.; Roy, R.; Holtom, G. R.; Xie, X. S. Imaging Chromophores with Undetectable Fluorescence by Stimulated Emission Microscopy. *Nature* **2009,** *461*, 1105–1109.

DOI: 10.1021/jz1014289 | *J. Phys. Chem. Lett.* **2010,** *1*, 3316–3322

(19) Boyer, D.; Tamarat, P.; Maali, A.; Lounis, B.; Orrit, M. Photothermal Imaging of Nanometer-Sized Metal Particles Among Scatterers. *Science* **2002,** *297*, 1160–1163.
(20) Uchiyama, K.; Hibara, A.; Kimura, H.; Sawada, T.; Kitamori, T. Thermal Lens Microscope. *Jpn. J. Appl. Phys.* **2000,** *39*, 5316–5322.
(21) Kukura, P.; Celebrano, M.; Renn, A.; Sandoghdar, V. Single-Molecule Sensitivity in Optical Absorption at Room Temperature. *J. Phys. Chem. Lett.* **2010**, *1*, 3323−3327.
(22) Gaiduk, A.; Yorulmaz, M.; Ruijgrok, P. V.; Orrit, M. Room-Temperature Detection of a Single Molecule's Absorption by Photothermal Contrast. *Science* **2010,** *330*, 353–356.
(23) Freudiger, C. W.; Min, W.; Saar, B. G.; Lu, S.; Holtom, G. R.; He, C.; Tsai, J. C.; Kang, J. X.; Xie, X. S. Label-Free Biomedical Imaging with High Sensitivity by Stimulated Raman Scattering Microscopy. *Science* **2008,** *322*, 1857–1861.
(24) Fu, D.; Ye, T.; Matthews, T. E.; Chen, B. J.; Yurtserver, G.; Warren, W. S. High-Resolution In Vivo Imaging of Blood Vessels without Labeling. *Opt. Lett.* **2007,** *32*, 2641–2643.
(25) Berciaud, S.; Lasne, D.; Blab, G. A.; Cognet, L.; Lounis, B. Photothermal Heterodyne Imaging of Individual Metallic Nanoparticles: Theory versus Experiment. *Phys. Rev. B* **2006,** *73*, 045424.
(26) Ahmadi, T. S.; Logunov, S. L.; El-Sayed, M. A. Picosecond Dynamics of Colloidal Gold Nanoparticles. *J. Phys. Chem.* **1996,** *100*, 8053–8056.
(27) Hodak, J. H.; Martini, I.; Hartland, G. V. Spectroscopy and Dynamics of Nanometer-Sized Noble Metal Particles. *J. Phys. Chem. B* **1998,** *102*, 6958–6967.
(28) Mian, S. M.; McGee, S. B.; Melikechi, N. Experimental and Theoretical Investigation of Thermal Lensing Effects in Mode-Locked Femtosecond Z-Scan Experiments. *Opt. Commun.* **2002,** *207*, 339–345.
(29) Fu, D.; Ye, T.; Grichnik, J.; Hong, L.; Simon, J. D.; Warren, W. S. Probing Skin Pigmentation Changes with Transient Absorption Imaging of Eumelanin and Pheomelanin. *J. Biomed. Opt.* **2008,** *13*, 054036.
(30) Denk, W.; Strickler, J. H.; Webb, W. W. Two-Photon Laser Scanning Fluorescence Microscopy. *Science* **1990,** *248*, 73–76.
(31) Alberto, D.; Giuseppe, C.; Maddalena, C. Two-Photon Fluorescence Excitation and Related Techniques in Biological Microscopy. *Q. Rev. Biophys.* **2005,** *38*, 97–166.
(32) Fu, D.; Ye, T.; Matthews, T. E.; Yurtsever, G.; Warren, W. S. Two-Color, Two-Photon, and Excited-State Absorption Microscopy. *J. Biomed. Opt.* **2007,** *12*, 054004.
(33) Hell, S. W.; Kroug, M. Ground-State-Depletion Fluorscence Microscopy: A Concept for Breaking the Diffraction Resolution Limit. *Appl. Phys. B: Laser Opt.* **1995,** *60*, 495–497.
(34) Gustafsson, M. G. L. Nonlinear Structured-Illumination Microscopy: Wide-Field Fluorescence Imaging with Theoretically Unlimited Resolution. *Proc. Natl. Acad. Sci. U.S.A.* **2005,** *102*, 13081–13086.

DOI: 10.1021/jz1014289 | *J. Phys. Chem. Lett.* **2010,** *1*, 3316–3322